AGU PUBLICATIONS

JGR

Journal of Geophysical Research: Biogeosciences

RESEARCH ARTICLE
10.1002/2013JG002317

Key Points:
- Scales of variability through temporal decomposition of hourly pCO_2
- Relationships between different pCO_2 temporal modes and some controlling factors
- Effect of sampling frequency on landscape studies and global balances

Supporting Information:
- Readme
- Figure S1
- Figure S2
- Figure S3

Correspondence to:
M. Morales-Pineda,
maria.morales@uca.es

Citation:
Morales-Pineda, M., A. Cózar, I. Laiz, B. Úbeda, and J. Á. Gálvez (2014), Daily, biweekly, and seasonal temporal scales of pCO_2 variability in two stratified Mediterranean reservoirs, *J. Geophys. Res. Biogeosci.*, *119*, 509–520, doi:10.1002/2013JG002317.

Received 19 FEB 2013
Accepted 15 FEB 2014
Accepted article online 20 FEB 2014
Published online 4 APR 2014

Daily, biweekly, and seasonal temporal scales of pCO_2 variability in two stratified Mediterranean reservoirs

María Morales-Pineda[1], Andrés Cózar[1], Irene Laiz[2], Bárbara Úbeda[1], and José Á. Gálvez[1]

[1]Department of Biology, University of Cadiz, Faculty of Marine and Environmental Sciences, Puerto Real, Cadiz, Spain, [2]Department of Applied Physics, University of Cadiz, Faculty of Marine and Environmental Sciences, Puerto Real, Cadiz, Spain

Abstract Temporal scales of variability for the partial pressure of CO_2 (pCO_2) in the surface waters of two stratified Mediterranean reservoirs were examined through the temporal decomposition of 5 month time series with hourly sampling frequency. pCO_2 time series included similar patterns of variability at daily, biweekly, and seasonal scales regardless of the difference in amplitude of the pCO_2 variation in the two reservoirs studied. Daily variability was strongly related to the day-night cycles of metabolic activity, accounting for about one third of the total amplitude in pCO_2 variation. At a biweekly scale, wind forcing led to higher rates of air-water CO_2 exchange and subsequently temporary partial mixing events associated to relevant increase of CO_2 concentration in surface waters. Seasonal variability accounted for one third of the amplitude of the pCO_2 variability and was coupled to the seasonal dynamics of water temperature and thermal stratification of the water column. Our results provide evidence that CO_2 emission from stratified water bodies shows significant variability at daily, biweekly, and seasonal scales; all of which should be taken into consideration in the analyses of the carbon fluxes. The wind-induced mixing events, operating at temporal scales between daily and seasonal cycles, may become a major factor controlling the pCO_2 dynamics. Hence, some of the most common models for computing CO_2 fluxes from pCO_2 were not able to reproduce the biweekly response patterns of CO_2 emissions to wind forcing.

1. Introduction

Carbon dioxide concentrations in inland waters are generally not in equilibrium with the atmosphere. Most of the freshwater systems are supersaturated in CO_2 and consequently act as CO_2 sources to the atmosphere, thereby playing an important role on greenhouse gases emissions [*Cole et al*., 1994; *Kling et al*., 2000; *Sobek et al*., 2005; *Tranvik et al*., 2009]. Artificial water reservoirs are water storage systems which can significantly alter the processing and fate of carbon in the watershed [*St Louis et al*., 2000; *Cole et al*., 2007; *Tranvik et al*., 2009]. The flux of carbon from reservoirs to the atmosphere is significant at the global scale, estimated at 0.3 Gt yr^{-1} [*St Louis et al*., 2000]. However, reservoirs emissions are still poorly known, partly because they greatly vary between regions and reservoir types [*Barros et al*., 2011]. While most of the research dealing with freshwater systems has traditionally been focused on lakes and hydroelectric reservoirs [*St Louis et al*., 2000; *Teodoru et al*., 2010; *Roland et al*., 2010], there is an increasing interest in studying water-supply, agricultural, and irrigation reservoirs, usually showing higher carbon emissions [*Downing et al*., 2008]. These types of reservoirs are particularly abundant in the Mediterranean region, where they are commonly used to collect, store, and manage the fluctuating water supply [*Nasseli-Flores*, 2003].

Multiple factors drive CO_2 concentrations in surface waters of aquatic systems. CO_2 supersaturation is commonly related to biological activity, as a result of a negative balance between photosynthesis and respiration in the water column [*del Giorgio et al*., 1997; *Sobek et al*., 2005] at daily scales. At longer time scales, abiotic factors may control surface CO_2 concentrations through the CO_2 inflow from surface and groundwater and high rain discharges, [*Jonsson et al*., 2007], photochemical reactions [*Bertilsson and Tranvik*, 1998], and water column mixing [*Baehr and DeGrandpre*, 2004]. All these and other processes simultaneously act at temporal scales spanning from days to years [*Kara et al*., 2012]. Long-term and high-frequency observations are critical for assessing pCO_2 dynamics and the processes underlying them. In this regard, autonomous biogeochemical sensors are able to provide long data series with unprecedented high frequency [*Hanson et al*., 2006], along spatial [*Van de Bogert et al*., 2012] and temporal variability [*Hanson et al*., 2006].

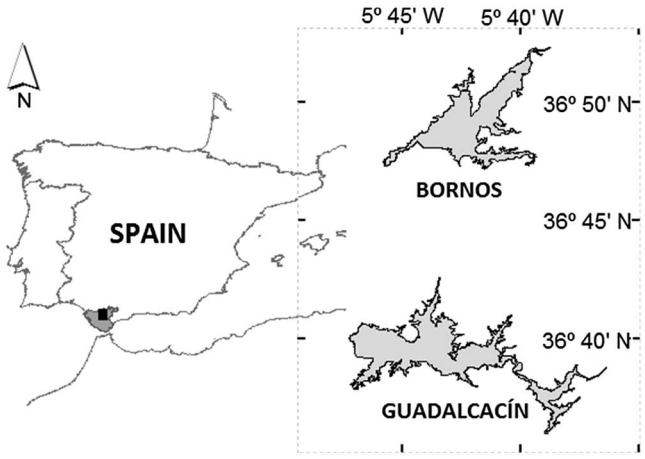

Figure 1. Location of the study reservoirs.

The first studies reporting high-frequency CO_2 measurements confirmed that variability in pCO_2 and CO_2 fluxes is high, being related not only to metabolic changes but also to physical forcing factors [*Baehr and DeGrandpre*, 2004]. The physical environment of the surface waters of lakes and reservoirs is the result of the dynamic interplay of wind stress, heating and cooling by solar radiation, and exchange with the atmosphere. Consequently, these processes influence the pCO_2 surface dynamics at different scales. Many reports have stressed the importance of high-frequency time series to explore the CO_2 dynamics in freshwater systems and the multi-scale forcing [e.g., *Jennings et al*., 2012; *Kara et al*., 2012]. However, the significance of the variability scales intervening on the pCO_2 time series as well as their relationships with the different forcing factors remain still unclear.

These observations raise two main questions: What is the importance of physical factors importance and timing over the observed variability? and, What is the main timing for each possible forcing factor? In the present study, we examine hourly series of pCO_2 in two Mediterranean reservoirs to analyze the relationship between the different pCO_2 temporal modes and potential controlling factors. We hypothesized that pCO_2 variability and consequently changes in the air-water CO_2 fluxes could be explained by a combination of forcing factors that influence both the community metabolism as well as the physical structure such as radiation, wind stress, and temperature. All these drivers vary at the daily scale and could affect pCO_2 variability with the possibility of different effects emerging at longer time scales (e.g., weeks, seasons). In order to assess the pCO_2 variability across different temporal scale we used decomposition methods and wavelet analysis of the temporal series. We also examined the role of biotic and abiotic processes, including solar radiation and wind, thermal and mixing conditions of the water column, and community metabolism, on the temporal variability of the CO_2 concentration of the surface waters. Finally, we discuss the general implications of the temporal scales of pCO_2 variability on the study of the CO_2 fluxes in stratified water bodies.

2. Material and Methods

2.1. Study Sites

The present study was conducted in two Mediterranean monomictic reservoirs located in the Guadalete river basin (southern Spain), namely Guadalcacín and Bornos (Figure 1). Guadalcacín reservoir (36°40′03.81″N–5° 47′05.20″W) has a surface area of 36.70 km^2, a maximum capacity of 853×10^6 m^3, and a maximum depth of 60 m. According to total phosphorus (TP) concentrations during the study period, it showed a mesotrophic status. Dissolved organic carbon (DOC) concentration was 3.9 ± 0.8 mg L^{-1} [*Romero-Martínez et al*., 2013] and 2.1 ± 0.6 μg L^{-1} of chlorophyll (Chl) (Table 1). On the other hand, Bornos reservoir (36°47′27.19″N–5° 45′37.74″W) is a eutrophic reservoir with higher TP, nitrate, and chlorophyll concentrations (Table 1). It has a surface of 23.41 km^2, 215×10^6 m^3 of maximum capacity, and a maximum depth of 22 m. The average DOC concentration during the study period in this reservoir was 6.1 ± 2.5 mg L^{-1}, being slightly higher than in Guadalcacín [*Romero-Martínez et al*., 2013]. Both reservoirs are used for irrigation, and Guadalcacín reservoir is also used for water supply. The hydrological behavior of both reservoirs is mainly characterized by the high variability of the Mediterranean climate, with extremely dry summers. The main characteristics of the reservoirs are summarized in Table 1.

2.2. pCO_2, Air-Water CO_2 Fluxes (F_{CO2}) and Temperature Measurements

A SAMI-CO_2 (Submersible Autonomous Moored Instrument for CO_2) sensor for pCO_2 was deployed at 2 m depth close to the dam, in the deepest part of the reservoirs. The sensor technical characteristics are

Table 1. Location and General Features of Guadalcacín and Bornos Reservoirs

Reservoir	Guadalcacín	Bornos
Latitude	36°40′03.81″N	36°47′27.19″N
Longitude	5°47′05.20″W	5°45′37.74″W
Capacity (hm^3) [a]	853	215
Watershed area (km^2)[a]	687	1344
Reservoir area (km^2) [a]	36.70	23.41
Water storage percent [bd]	32.5	97.42
Maximum depth (m) [d]	60	22
Annual mean precipitation (mm) [a]	631	746
Annual mean air temperature (°C) [c]	17.7	17.7
Precipitation (mm) [cd]	52.6	181.1
Mean air temperature (°C) [cd]	23.5 ± 3.5	23.6 ± 4.6
DOC ($mg\,L^{-1}$) [d]	3.9 ± 0.8	6.1 ± 2.5
Chl ($\mu g\,L^{-1}$) [d]	2.1 ± 0.6	7.0 ± 5.0
TP ($mg\,P\,m^{-3}$) [d]	30.7 ± 10.0	53.7 ± 113.5
Nitrate ($mg\,NO_3^-\,L^{-1}$) [d]	2.3 ± 0.7	8.2 ± 3.1
Trophic status	Mesotrophic	Eutrophic

[a]Guadalquivir Hydrographic Confederation.
[b]Andalusia Regional Environment Department (http://www.juntadeandalucia.es/medioambiente).
[c]Spanish Meteorological Agency (AEMET).
[d]Study period.
Mean ± standard deviation is shown in some limnological variables for the study period.

described by *DeGrandpre et al.* [1995, 1997]. The SAMI-CO_2 was programmed to acquire data every hour and was calibrated prior to deployment using CO_2 gas standards [*DeGrandpre et al.*, 1997]. Measurement precision, estimated from the SAMI-CO_2 calibrations, was ± 1 μatm at 360 μatm, ± 10 μatm at 1200 μatm, and ± 20 μatm at 1500 μatm. The increasing uncertainty is related to the decrease in sensitivity at higher pCO_2 levels [*DeGrandpre et al.*, 1999]. Accuracy during the deployment was determined by estimating pCO_2 from pH and total alkalinity (TA) using CO_2 equilibrium software [CO2SYS, *Lewis and Wallace*, 1998] and the dissociation constants for freshwater provided by *Millero* [1979]. TA was measured by potentiometric titration using Metrohm 808 (Tiamo, 1.2 version) and adding 0.1 N HCl until a stable pH 4.5 was reached. Calculated and in situ pCO_2 measurements agreed to within ± 6.7% ($n = 9$) in Guadalcacín and ± 7.25% ($n = 11$) in Bornos (Figure 2). The same tendency was followed between pCO_2 calculated and SAMI-CO_2 measurements. The SAMI-CO_2 was deployed in Guadalcacín reservoir during summer 2009 (from 5 May to 15 October 2009), and in Bornos reservoir, during summer 2010 (from 15 May to 25 October 2010). Temperature (±0.001°C) was also registered by the SAMI-CO_2 sensor.

F_{CO2}, in $mmol\,C\,m^{-2}\,d^{-1}$, was modeled following the concentration gradient between the water and the air using the equation:

$$F_{CO2} = \alpha\, k\left([CO_2]_{water} - [CO_2]_{sat}\right)$$

where α is the chemical enhancement factor of the air-water flux of CO_2, calculated from the theoretical model of Hoover and Berkshire (1969) as described in *Wanninkhof and Knox* [1996]; k is the gas transfer velocity ($cm\,h^{-1}$) estimated from wind speed at 10 m height (U_{10} in $m\,s^{-1}$); $[CO_2]_{water}$ is the CO_2 concentration in the water ($\mu atm\,L^{-1}$); and $[CO_2]_{sat}$ is the CO_2 concentration at equilibrium with the atmosphere, calculated from Henry's constant [*Weiss*, 1974] considering a mean of pCO_2 in equilibrium with the atmosphere of 379 μatm [*IPCC*, 2007]. Gas transfer velocity was calculated estimated from U_{10} ($m\,s^{-1}$) using two different models: *Cole and Caraco* [1998] and *Crusius and Wanninkhof* [2003] bilinear approximation.

Temperature profiles were determined with a serial chain of ONSET HOBO thermistors with 30 min frequency during the whole studied period. In summer 2009, the maximum depth in Guadalcacín reservoir was around 30 m, and nine thermistors were installed at 0, 2, 5, 8, 11, 13, 16, 21, and 25 m. In summer 2010, the depth in Bornos reservoir was around 20 m, and hence, seven thermistors were deployed at 0, 2, 5, 8, 11, 14, and 18 m depth.

2.3. Meteorological Data

Hourly air temperature and wind speed were measured from the nearest meteorological station (36° 39′49.31″N, 5°47′0.53″W), situated 200 m from Guadalcacín mooring site and 14 km from Bornos reservoir. Solar radiation (200–2500 nm) was measured from a meteorological station (36°45′02″N, 6°32′12″W) located at 26 and 28 km distance from Guadalcacín and Bornos, respectively. This information was provided by the Spanish Meteorological Agency (AEMET).

2.4. Data Calculations

Mixing depth (Z_{mix}) was calculated following *Staehr et al.* [2012] and was determined every 30 min from the thermistor chain data. The measured temperature profiles were implemented in a model [*Rimmer et al.*, 2005] that generates a high-resolution profile (0.1 m) of temperature. From those profiles, density gradients were

calculated. The water column was considered stratified when the density gradient exceeded 0.07 kg m^{-3} m^{-1} [*Read et al.*, 2011; *Sadro et al.*, 2011] and unstable below this value. Short-term microstratifications in the uppermost water layers, which occurred occasionally during daytime, were disregarded.

2.5. Statistical Methods

Different approaches were used to analyze the data in order to distinguish and extract the best frequencies for each physical forcing factor over the pCO_2 original time series. First, a cross-wavelet transform (XWT) analysis was carried out to examine linkages between each of the environmental variables considered (x_n, that in this case were: solar radiation, wind speed, and water temperature) and pCO_2 time series (y_n) at the two locations under study. The XWT analysis is constructed from the continuous wavelet transform (CWT) of each of the time series (x_n and y_n) and is defined as $W^{XY} = W^X W^{Y*}$, where W^X and W^Y represent the CWT of time series x_n and y_n, respectively, and * denotes complex conjugate [*Grinsted et al.*, 2004]. The choice of the appropriate mother wavelet depends on the nature of the signals and on the type of information to be extracted from them [*Torrence and Compo*, 1998]. Here, we focused on identifying regions in the time frequency space where each pair of time series showed high common power. For this purpose, the Morlet mother wavelet was used because it provides a better frequency resolution, and thus, it can identify periodic signals more accurately than other wavelets [*De Moortel et al.*, 2004]. The cross-wavelet power spectrum (XWPS) was calculated from the XWT results in order to estimate the covariance between each pair of time series as a function of frequency. The statistical significance was estimated using Monte Carlo methods. All the analyses were carried out using a Matlab 7.0 software package (MathWorks 2002) developed and freely distributed by *Grinsted et al.* [2004]. In addition, a spectral analysis [*Emery and Thomson*, 2004] was carried out for each time series in order to identify and interpret the energy bands of high common power obtained with the XWT.

Based on the XWT results, all the time series were filtered using a band-pass fast Fourier transform filter in order to isolate the corresponding frequency bands of high common power detected by the XWT analysis. Finally, each pair of filtered time series was compared by performing time-lagged linear correlations between them. In order to account for autocorrelation in the data, the effective number of degrees of freedom (EDOFs) was calculated using the definition of the integral time scale as in *Emery and Thomson* [2004]. The EDOFs were then used to re-compute the *p*-value and the 95% confidence limits of the correlation, *R*; the later were obtained based on the transformation of *R* into the standard normal variable which is normally distributed and has a known standard error of $1/\sqrt{N-3}$, *N* being the EDOFs [*Emery and Thomson*, 2004]. For each case, the correlation at zero lag was compared with the maximum correlation obtained as in *Zar* [1999]. When the two correlation coefficients were not statistically different, the correlation at zero lag was selected; otherwise, the maximum correlation value was kept.

The second approach consisted in a decomposition of the original pCO_2 hourly series based on the dominant frequencies identified in the XWT and spectral analyses. A daily component (pCO_2^{daily}) was calculated by extracting the corresponding 24 h moving average (24 h_{avg}) of the observed pCO_2 time series (equation (1)). A biweekly component ($pCO_2^{biweekly}$) was calculated through the extraction of biweekly moving average (bw_{avg}) from the 24 h moving average (equation (2)). The seasonal component ($pCO_2^{seasonal}$) was calculated by extracting the pCO_2 time series data average ($pCO_{2\ avg}$) from the biweekly moving average (equation (3)). Mathematically, these calculations can be expressed as:

$$pCO_2^{daily} = pCO_2 - 24h_{avg} \quad (1)$$

$$pCO_2^{biweekly} = 24h_{avg} - bw_{avg} \quad (2)$$

$$pCO_2^{seasonal} = bw_{avg} - pCO_{2\ avg} \quad (3)$$

Therefore, the pCO_2 hourly series may be described as:

$$pCO_2 = pCO_{2\ avg} + pCO_2^{seasonal} + pCO_2^{biweekly} + pCO_2^{daily} \quad (4)$$

3. Results

3.1. Data Overview

In total 6333 pCO_2 measurements at hourly resolution were gathered, 2977 in Guadalcacín reservoir during 2009 (126 days) and 3356 in Bornos reservoir during 2010 (148 days). pCO_2 measurements ranged from 391

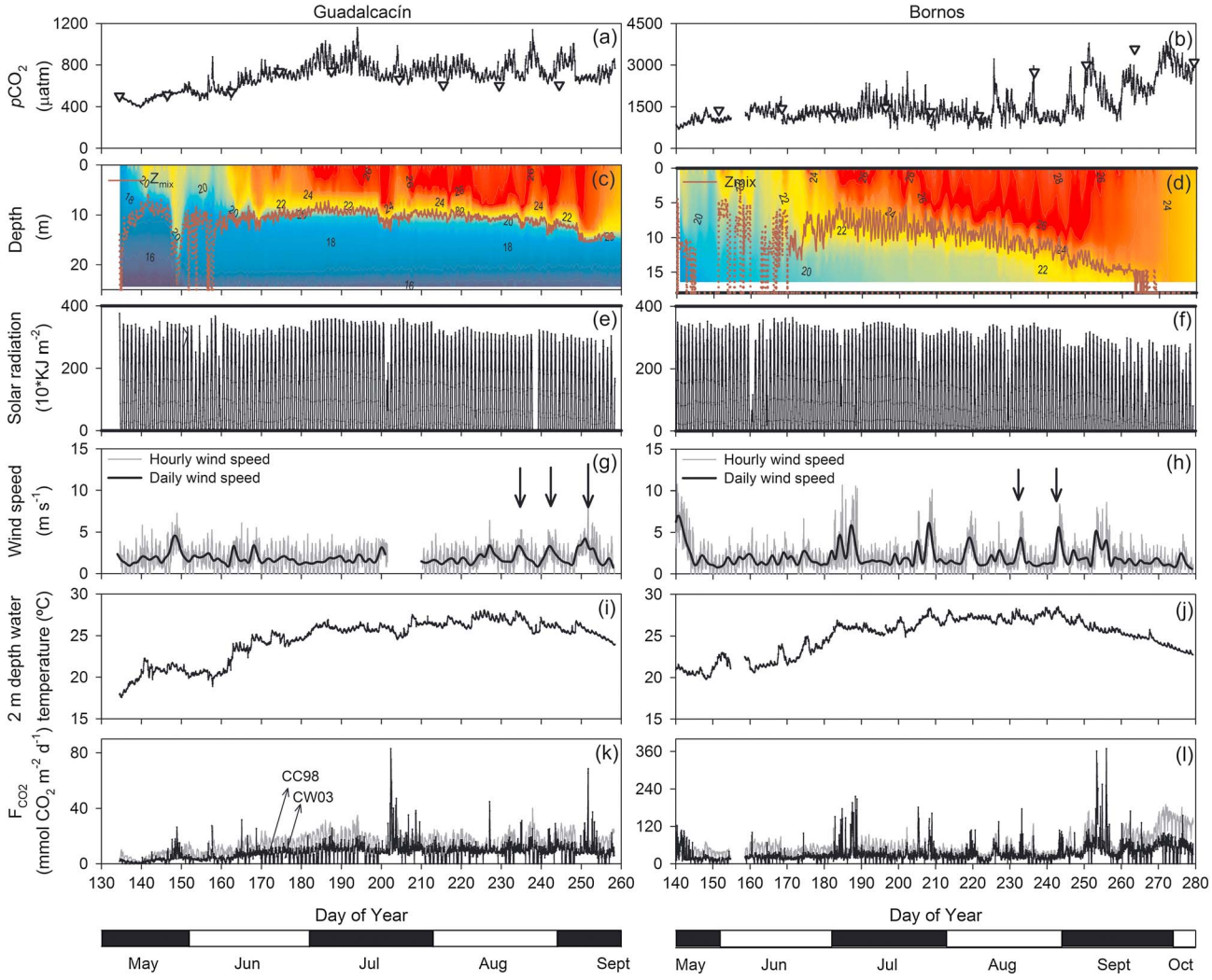

Figure 2. (a, b) Temporal variability of pCO_2, (c, d) mixing depth, (e, f) solar radiation, (g, h) wind speed, (i, j) surface water temperature, and (k, l) air water fluxes in (left panels) Guadalcacín reservoir and (right panels) Bornos reservoir. Sample measurements at 2 m (open triangles) data quality verification are also shown (see Material and Methods). Mixing depth (Z_{mix}) is shown with red line on a contour plot of water temperature (°C). Dashed red line indicates the period of higher water column instability while continuous red line indicates stratification period. Grey line contours represents water temperature (°C) in 1°C intervals. The grey line corresponds to *Cole and Caraco* [1998] power relationship (CC98) and the black line to the *Crusius and Wanninkhof* [2003] bilinear relationship (CW03). Black arrows indicate high wind speed events (see discussion).

to 1160 µatm in Guadalcacín and from 652 to 3840 µatm in Bornos. The averages (±SD) for the whole study periods were 695 ± 129 µatm and 1529 ± 633 µatm in Guadalcacín and Bornos, respectively (Figures 2a and 2b). Both reservoirs were supersaturated throughout the study. The mean amplitude of the diel changes in pCO_2 was 144 µatm (range, 12 to 457 µatm) in Guadalcacín, while it was 657 µatm (range, 80 to 2044 µatm) in Bornos. At the daily scale, minimum pCO_2 values were found between 15:00 and 18:00 h and maximum pCO_2 values between 22:00 h and 06:00 h (Figure S01).

Estimates of carbon emission, as CO_2 to the atmosphere, were considerably different depending on the model used, although it was consistent that total carbon emission was fourfold higher in Bornos than in Guadalcacín (Figures 2k and 2l). Applying the model proposed by *Cole and Caraco* [1998], CO_2 emission ranged from 0.0 to 40.2 mmol C m^{-2} d^{-1} in Guadalcacín (mean = 12.5 ± 6.2 mmol C m^{-2} d^{-1}), whereas it ranged from 0.0 to 82.8 mmol C m^{-2} d^{-1} (mean = 8.0 ± 6.5 mmol C m^{-2} d^{-1}) following *Crusius and Wanninkhof* [2003]. In the Bornos, CO_2 emission ranged from 8.3 to 190.5 mmol C m^{-2} d^{-1} (mean = 50.0 ± 33.1 mmol C m^{-2} d^{-1}) following *Cole and Caraco* [1998], and from 0.0 to 368.3 mmol C m^{-2} d^{-1} (mean = 33.0 ± 30.6 mmol C m^{-2} d^{-1}) following *Crusius and Wanninkhof* [2003].

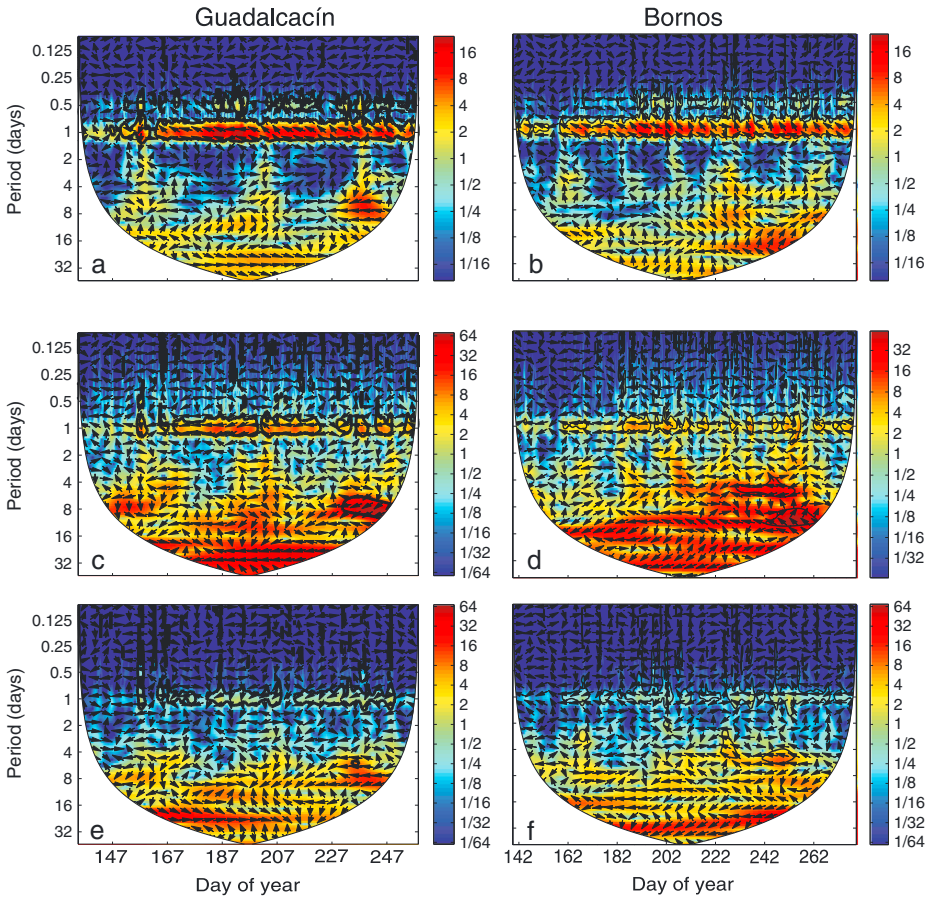

Figure 3. Cross-wavelet power spectrum (XWPS) of (a, b) solar radiation, (c, d) wind speed, and (e, f) water temperature with pCO_2 in (left panels) Guadalcacín reservoir and (right panels) Bornos reservoir. Color contours represent cross-wavelet power and vectors indicate the relative phase relationship between the two time series (with in-phase pointing right, anti-phase pointing left, solar radiation or wind speed or water temperature/pCO_2 leading pCO_2/solar radiation or wind speed or water temperature by 90° pointing straight down/up). The 5% significance level is shown as a thick contour. White regions on either end indicate the "cone of influence," where edge effects become important.

Water temperature at surface (2 m depth) ranged from 17.6 to 28.5°C (mean, 24.5°C) in the Guadalcacín and from 16.8 to 28.5°C (mean, 24.7°C) in the Bornos reservoir. As expected, water temperature increased during late spring, was rather constant during summer, and decreased during early autumn in both reservoirs (Figures 2i and 2j). From beginning of June, the water column of both reservoirs was stratified. Thermal stratification persisted throughout the summer without any periods of complete mixing in Guadalcacín. In Bornos, however, Z_{mix} increased and reached the bottom at the end of the study period (September, Figure 2d).

Solar radiation showed strong diel changes with no significant differences in the daily amplitude during the study period (Figures 2e and 2f). Mean wind speeds were relatively low in both reservoirs (1.9 ± 1.3 m s^{-1} in Guadalcacín 2009 and 2.0 ± 1.6 m s^{-1} in Bornos) (Figures 2g and 2h). Strong wind events (wind speeds from 5 to 15 m s^{-1}) were more frequent in Bornos than in Guadalcacín. These sporadic events were related to southeasterly and easterly winds.

3.2. Time Series Analyses

Figure 3 shows the cross-wavelet power spectrum of solar radiation, wind speed, and water temperature with pCO_2, displayed as a function of period and time. Solar radiation (Figures 3a and 3b) showed significant and high common power (i.e., relationship) with pCO_2 at daily scale in both reservoirs from June. Before

Table 2. Correlation Parameters Between pCO_2 and Other Physical Variables Filtering at Different Time Scales

		pCO_2		
Reservoir		Daily freq (24 h) Solar radiation	Biweekly freq (10–16 days) Wind speed	Seasonal freq (90–125 days) Water temperature
Bornos	R	−0.87	−0.83	0.58
	p	0	0	0.13
	n (EDOFs)	549	45	8
	nseries	2332	2332	2331
	Time lag	2	0	0
Guadalcacín	R	−0.82	−0.89	0.98
	p	0	0	0
	n (EDOFs)	701	59	9
	nseries	2923	2725	2939
	Time lag	2	0	0

this month, there were two discontinuous patches of common power in the same band in Bornos (Figure 3b) and one in Guadalcacín (Figure 3a). The orientation of the phase arrow shows a negative correlation between the time series, with pCO_2 decreasing toward high solar radiation. Time series spectral analysis revealed that solar radiation presents the main energy peak at the daily scale, representing 75% and 82% of the energy peaks for Bornos and Guadalcacín, respectively. Based on these results, the series were filtered to isolate the daily periodicity and compared through a time-lag linear correlation, obtaining a negative relationship at this scale (Table 2), in agreement with the XWT results.

The XWPS of wind speed and pCO_2 (Figures 3c and 3d) showed discontinuous patches of common power in the daily band. These patches are larger in Guadalcacín (Figure 3c), pointing to a more stable relationship between wind speed and pCO_2. Thus, the wind spectra in Guadalcacín showed a peak containing 26% of the energy at this scale, while it only represented 9% of the energy in Bornos. Moreover, wind time series in Bornos showed frequent events of high wind speed related to decreases in pCO_2. A band of high and significant common power is found in the 5–6 day period between mid-August and mid-September only in Bornos. Finally, a band of high relationship in the 12 day period (roughly biweekly) is observed from July onward in both reservoirs, although it was significant only for a time period in September. This is consistent with the small energy peaks ($< 4\%$) observed for wind and pCO_2 spectra in both reservoirs at this time scale (Figure 3). The biweekly filtered series of pCO_2, wind speed, Z_{mix}, and F_{CO2} (using different models) for Guadalcacín and Bornos are shown in Figure 4. These showed a positive correlation between wind speed and Z_{mix}, and a negative correlation between wind speed and pCO_2 in both reservoirs (Table 2), in agreement with the orientation of the phase arrows obtained in the XWT analysis.

Discontinuous patches of low but significant relationship were observed at the daily period in the XWPS of water temperature and pCO_2 (Figures 3e and 3f). The spectra of both reservoirs also showed a large region of common power corresponding to a period of 30 days, although none of them was statistically significant. The spectral analysis of temperature and pCO_2 series showed that the monthly energy peaks were relatively small, containing about 5% of the energy in Bornos and 4% in Guadalcacín. Moreover, the spectra showed a

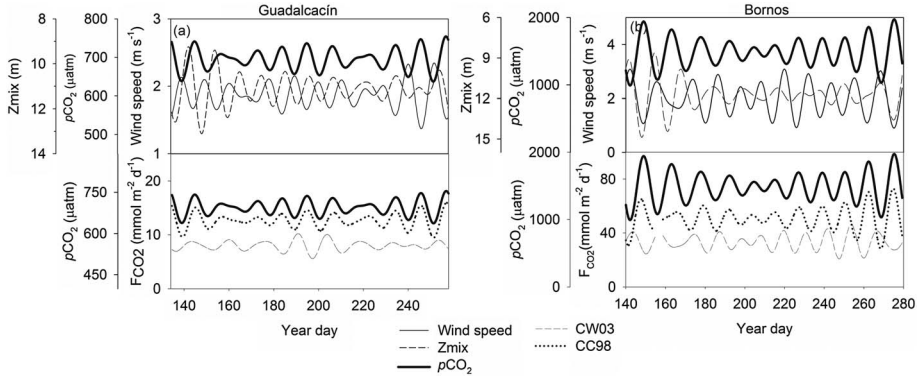

Figure 4. Time series filtrated at biweekly scale. pCO_2 (heavy line), wind speed (plain line), Z_{mix} (dashed line) for (left column, a) Guadalcacín and (right column, b) Bornos. The dotted line represents the *Cole and Caraco* [1998] relationship (CC98), and the short dash line represents the *Crusius and Wanninkhof* [2003] relationship (CW03).

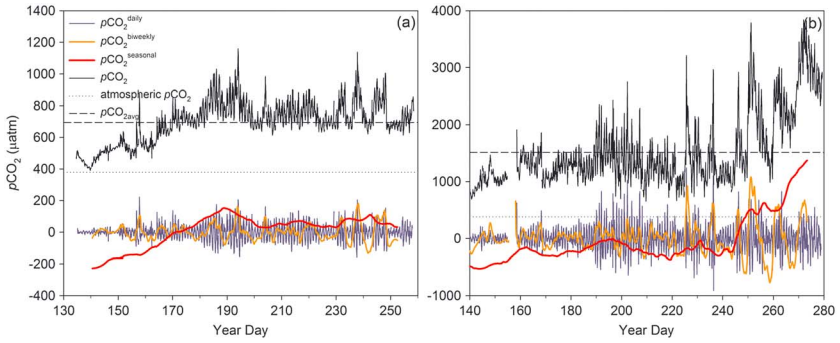

Figure 5. Decomposition of the original pCO_2 hourly series (black line) in (a) Guadalcacín reservoir and (b) Bornos reservoir. Daily (pCO_2^{daily}), biweekly ($pCO_2^{biweekly}$), and seasonal ($pCO_2^{seasonal}$) variability in pCO_2; pCO_2 observed data set (pCO_2) and pCO_2 average of the studied period (pCO_{2avg}). pCO_2^{daily}, $pCO_2^{biweekly}$, and $pCO_2^{seasonal}$ were calculated following the next equations: $pCO_2^{daily} = pCO_2 - 24h_{avg}$; $pCO_2^{biweekly} = 24h_{avg} - bw_{avg}$; $pCO_2^{seasonal} = bw_{avg} - pCO_{2avg}$ (see Material and Methods).

large semi-annual peak (90 to 125 days), containing between 20% and 80% of time series energy in Bornos and between 40% and 67% in Guadalcacín. We tried to increase the width of the Morlet wavelet in order to cover the semiannual period and, although a continuous band of high and significant common power was found in the semi-annual band (not shown here), the analysis fell outside the cone of influence. This indicates that the length of the time series was too short (about 4.7 months) in relation to the chosen width of the wavelet, and this signal should not be explored with the XWT analysis. Using the decomposition analysis, we found a statistically positive correlation between the seasonal components of pCO_2 and water temperature (Table 2).

The influence of different time scales on the variability of the original pCO_2 hourly series was also estimated from the temporal decomposition analysis. Daily variability was mainly related to solar radiation (Figures 3a and 3b) and accounted for about 30% of the variability in the pCO_2 hourly series in both reservoirs. The influence of the biweekly variability on pCO_2 variability was 2 to 3%, according to the XWT (Figures 3c and 3d) and correlation analyses (Table 2). This scale of variability was mainly related to high wind speed events. Finally, the seasonal period accounted for 68% of the variability of the original pCO_2 series and was mainly related to the water temperature.

The relative contribution of each temporal component ($pCO_2^{seasonal}$, $pCO_2^{biweekly}$, pCO_2^{daily}) to the total amplitude of the temporal variability in pCO_2 was also calculated (Figure 5). In Guadalcacín, the seasonal component accounted for 34% of the amplitude of the pCO_2 variability; the biweekly component for 28%; and the daily component for 39%. In Bornos, the seasonal component accounted for 32%, the biweekly component for 31%, and the daily component for 36% of the amplitude of the pCO_2 variability.

We must also note that small repeated decreases of pCO_2 were observed only after mid-night at hourly scale. These pCO_2 dips were found between 22:00 and 05:00 h, with a median at 03:00 h in Bornos and at 02:00 h in Guadalcacín (Figure 6). A post-midnight pCO_2 dip was observed in Guadalcacín in 46% of the days studied, which ranged from 8 to 162 µatm (mean 46 µatm). In Bornos, 63% of the days showed similar pCO_2 dips, ranging between 14 and 993 µatm (mean 199 µatm).

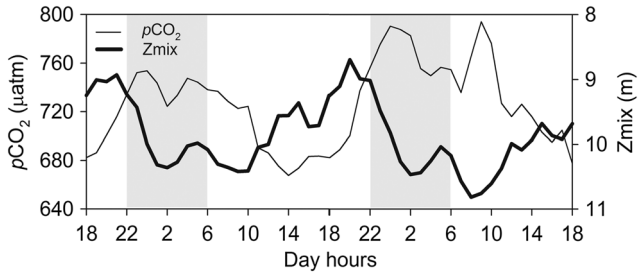

Figure 6. A 3 days period (18:00 27 June to 18:00 29 June) in Guadalcacín reservoir for pCO_2 (black curve) and Z_{mix} (heavy black). Shadow represents nights hours.

4. Discussion

Environmental forcing factors (e.g., solar irradiance, wind, and temperature) drive the pCO_2 dynamics in surface waters through their control on physical, chemical, and biological processes at different time scales. In the present work, we used temporal series statistics and modeling to link the timing of the environmental forcing factors with their relative importance over the CO_2 dynamics. Results show that surface water pCO_2 in reservoirs can significantly vary at daily, seasonal as well as biweekly scales.

The daily component (pCO_2^{daily}) explained around 30% of the amplitude of temporal variability in the original pCO_2 series. The relevance of the daily component was similar in both reservoirs in spite of the differences in amplitude of the pCO_2 diel cycles in the two reservoirs studied (Figure 5). We found significantly ($p < 0.05$) higher diel variations in Bornos, in agreement with those systems characterized by high nutrients concentrations and high metabolic fluxes [*Hanson et al*., 2003]. The observation of relatively low diel variations in surface pCO_2 in Guadalcacín is also consistent with previous results from other low-productivity systems [*Finlay*, 2003], where plankton metabolic activity may be strongly constrained by the resource availability.

A major environmental factor driving phytoplankton activity at daily scale is solar radiation; accordingly, a negative correlation was found between radiation and pCO_2 at daily time scales (Table 2). This result agrees with studies linking diel changes of CO_2 concentration with PAR and metabolism as result of the strong control of PAR on the balance between production and respiration at this time scale [*Carignan*, 1998; *Hanson et al*., 2006 and *Huotari et al*., 2009]. Respiration processes widely dominate plankton metabolism during nighttime, leading to an increase of pCO_2 in the epilimnion. The correlation between radiation and pCO_2 had a time lag of 2 h (Table 2), probably due to the delay in the response of the community metabolism. Convective processes in the water column may also significantly affect the pCO_2 dynamics at daily scale. High surface CO_2 fluxes have been measured during periods of convective mixing, which often occur at night, when cooling of the surface water induces vertical water movements and upwelling of deep CO_2-rich water [*Åberg et al*., 2010; *Eugster et al*., 2003]. In our study reservoirs, we found frequent hourly dips in pCO_2 during the nighttime (Figure 6). These results could be explained by a convective circulation into the epilimnion, resulting in a deepening of a poor CO_2 surface water layer to the depth (2 m) at which the SAMI-CO_2 sensor was located. Similar observations were recorded in lakes that used high-frequency oxygen sensors to detect a midnight oxygen surge (T. Kratz, personal communication). Thus, the hourly variation of surface CO_2 concentration at daily scale would result from a combination of biological processes (i.e., diel cycles of metabolic balance) as well as short-term hydrodynamic processes (i.e., night convection).

At biweekly scale, wind speed was the most evident forcing factor. A negative relationship was found between pCO_2 and wind speed (Table 2 and Figure 4). Surface pCO_2 may directly decrease due to the acceleration of the exchange of water dissolved gases with the atmosphere. Likewise, wind-induced mixing may lead to the entrainment of nutrients into the epilimnion and subsequent production. Nevertheless, the regression between pCO_2 and wind speed was maximal without time lag, suggesting that the acceleration of the CO_2 exchange was the main process acting at this scale. Using maximum wind speed events corresponding to pCO_2 drop periods, CO_2 fluxes to the atmosphere estimated from *Crusius and Wanninkhof* [2003] model were enough to explain the pCO_2 declines measured in the surface waters of both reservoirs (i.e., Guadalcacín, 211 μatm, period: 233–236 days; Bornos, 1802 μatm, period: 253–259 days) (Figure S02), also supporting air-water gas exchange as the main process driving these pCO_2 decreases.

On the other hand, we registered some episodes of high wind speed related to subsequent increases in pCO_2. In these episodes, CO_2 concentrations in the surface water increased because the downward epilimnion expansion was large enough to facilitate the release of CO_2 pools contained in the hypolimnion. As the mixing depth stabilized and CO_2 concentration into the epilimnion became smaller, surface pCO_2 decreased regularly until a new equilibrium was reached. Bornos showed particularly high significant common power in the XWPS due to these episodes (Figures 3c and 3d). Indeed, the largest CO_2 emissions were related to events of intense deepening of the mixing layer (Figure S02). In Guadalcacín, the significance of these episodes was lower, although an increase in wind speed and mixing depth was also found at the end of the study period (Figure 2g, arrows). These strong-mixing episodes highlight the fact that CO_2 generated by respiration in sediments and trapped in deep waters under the thermocline can be finally released to the water column and to the atmosphere as a carbon flux.

Modeling of the air-water fluxes (F_{CO2}) from pCO_2 provides useful information on the carbon budgets in water bodies. The models of *Cole and Caraco* [1998] (CC98) and *Crusius and Wanninkhof* [2003] (CW03) are the most

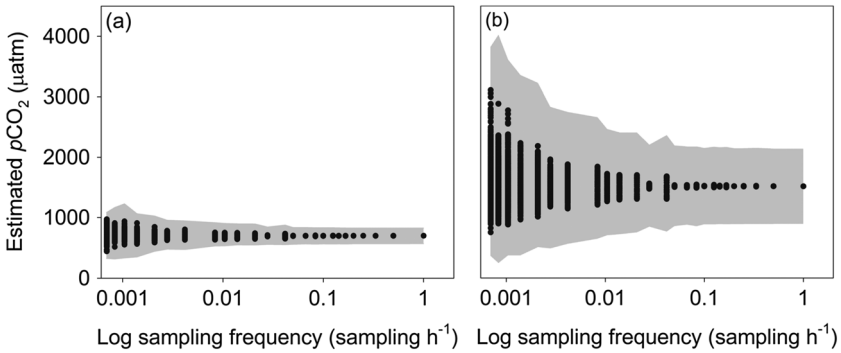

Figure 7. The effect of different sampling frequencies on pCO_2 (black circles) and the corresponding standard deviation (SD, grey) in (a) Guadalcacín and (b) Bornos reservoirs.

widely used models for F_{CO2} calculations, and both of them are based on empirical relationships between wind speed and gas transfer velocity (k). Applying CC98 model to our data at biweekly scale, we found a positive correlation between wind speed and *k*, and a negative correlation between wind speed and F_{CO2} (Figure 4 and Figure S02). In contrast, the CW03 model showed increases of F_{CO2} as the wind speed increased, in agreement with the observed decreases of surface CO_2 concentration.

Turbulence is a key factor driving gas exchange across the air–water interface because it constitutes a direct proxy of the physical state of the mass boundary layer [*Tokoro et al.*, 2008]. *Vachon et al.* [2010] pointed out the difficulty of choosing a suitable transfer velocity (*k*) value. The uncoupling found between the two-modeled F_{CO2} highlights the relevance of the selection of the function relating *k* and wind speed. In systems where wind forcing becomes important, CW03 model seems to be more accurate for modeling F_{CO2} dynamics since it relates windy events with decreasing pCO_2, and increasing in F_{CO2}. This process was not well reproduced with CC98 in our data (Figure S03).

Overall, the relative contribution of the biweekly component on the total amplitude of pCO_2 was approximately one third in both reservoirs. The main differences observed between reservoirs was related to the larger maximum amplitude found in Bornos (1853 µatm) at biweekly scales when compared to that of Guadalcacín (313 µatm) (Figure 5, $pCO_2^{biweekly}$).

Water temperature was closely related to the seasonal pCO_2 variability ($pCO_2^{seasonal}$; Figure 5), explaining 68% of the total hourly pCO_2 variability and accounting for one third of the total maximum amplitude of *p*CO2. The positive relationship between temperature and pCO_2 (Table 2) could be explained by the temperature effect on CO_2 solubility and/or metabolic rates. The large percentage of total variability explained by the seasonal trend of surface temperature stresses the role played by seasonal scale processes on the pCO_2 dynamics. In both reservoirs, pCO_2 showed a progressive increase with the warming up of the water column. At the end of the summer period and coinciding with the seasonal cooling (Figure 2; Bornos), a change in the seasonal trend of pCO_2 was found. This event was likely associated to the release of the CO_2 pools accumulated in the hypolimnion during the stratification [*Jonsson et al.*, 2007].

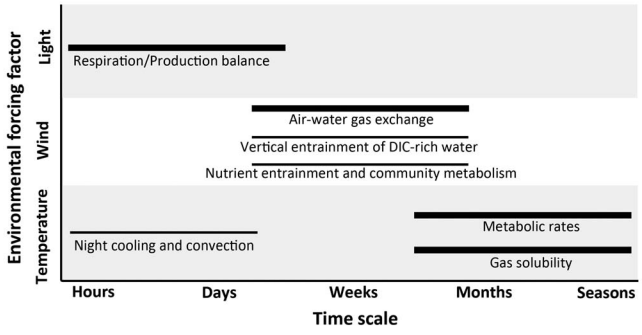

Figure 8. Conceptual diagram of the main processes acting on the surface pCO_2 dynamics of the reservoirs studied in relation to the time scale and the environmental forcing factors.

Respiration and production rates in aquatic ecosystems have been reported to be temperature dependent [*Durocher et al*., 2012; *Hoppe et al*., 2002; *del Giorgio and le B. Williams*, 2005]. An analysis of the pCO_2 variation in lakes showed that temperature does not exert an important role on pCO_2 dynamics [*Sobek et al*., 2005], whereas other variables such as DOC were major regulators of pCO_2. More recently, *Hanson et al*. [2006] showed that temperature dependence is higher at longer time scales, significantly affecting the final pCO_2 variability. Globally, seasonal variations in temperature are more remarkable in boreal and temperate regions than in tropical ones. This latitudinal pattern is coupled to the observed patterns of greenhouse gas emissions from reservoirs [*Barros et al*., 2011; *Takahashi et al*., 2002]. Although pCO_2 is not a direct measure of the CO_2 flux from the waterbodies, it is the most important factor influencing these emissions [*Sobek et al*., 2005]. Given the strong influence of the seasonal trend of temperature on pCO_2 (Table 2), our results suggest that the predicted rise in temperature [*IPCC*, 2007] may have a relevant impact on pCO_2 and, consequently, on CO_2 emissions.

In order to demonstrate the importance of considering the different scales of variability in the assessment of CO_2 fluxes within stratified water bodies, a sensitivity test was performed by varying the sampling frequency from one per hour up to six per year (Figure 7). The standard deviation (SD) of the pCO_2 averages considerably increased with low sampling frequencies, although deviations were considerably lower in Guadalcacín, the reservoir with lower trophic status, and smaller amplitude in the pCO_2 variations (Figure 7). Interestingly, the sampling frequency considerably affects the pCO_2 means when night values are not taken into account. Although the hourly change in pCO_2 in oligotrophic or mesotrophic freshwaters is apparently small, the importance of accounting for night variability in each 24 h period should not be overlooked. Night pCO_2 values from 22:00 h to 06:00 h were higher than the daily averages (Figure S01); hence, sampling only during light hours leads to an underestimation of daily pCO_2.

We must note that the estimation of F_{CO2} from pCO_2 measurements is subject to the accumulation of errors along the modeling process. Hence, uncertainties would increase for longer F_{CO2} time series. Moreover, the sensitivity test showed that uncertainty is higher for the averaged estimates of F_{CO2} than pCO_2.

5. Conclusions

There is an increasing consensus that reservoirs contribute significantly to global anthropogenic CO_2 emissions. Our study stresses the importance of considering different time scales when assessing the role of reservoirs on the carbon cycle. Cross-wavelet and decomposition analyses of pCO_2 time series unraveled at scales of variability the environmental forcing factors act. The results allowed for identifying the main forcing factors and processes controlling the CO_2 dynamics (Figure 8). Notwithstanding the differences in amplitude of the pCO_2 temporal variability of the reservoirs studied, the relative contribution of each different temporal component (daily, seasonal, and biweekly) to the total amplitude was similar.

Since the existing models that estimate F_{CO2} from pCO_2 measurements provide different response patterns to windy episodes, the estimates of air-water fluxes should be treated with caution. The relationship of gas transfer velocity with wind speed should be carefully assessed to improve the reliability of the models. Finally, our analysis demonstrates that there is a considerable loss of accuracy in the F_{CO2} estimates as sampling frequency decreases.

Acknowledgments

This work has been supported by the Spanish Ministry of Science and Innovation (MICINN) through the SEDICO project (ref. CGL2007-64729). M. Morales-Pineda was financially supported by the Spanish Ministry of Science and Innovation through the FPI fellowship program (BES2008-008160). The authors are thankful to S. Sobek for his valuable comments, and B. Obrador, D. Vachon, L. Romero-Martínez, and the reservoir staff, especially Jesús A. Muñoz and B. Caballero, are also acknowledged for their assistance during the whole sampling period. We also thank two anonymous reviewers for their constructive suggestions. Meteorological data were provided by the Spanish Meteorological Agency (AEMET).

References

Åberg, J., M. Jansson, and A. Jonsson (2010), Importance of water temperature and thermal stratification dynamics for temporal variation of surface water CO_2 in a boreal lake. *J. Geophys. Res.*, *115*, G02024, doi:10.1029/2096JG001085.

Baehr, M. M., and M. D. DeGrandpre (2004), In situ pCO_2 and O_2 measurements in a lake during turnover and stratification: Observations and modeling, *Limnol. Oceanogr.*, *49*(2), 330–340.

Barros, N., J. J. Cole, L. T. Tranvik, Y. T. Prairie, D. Bastviken, V. L. M. Huszar, P. del Giorgio, and F. Roland (2011), Carbon emission from hydroelectric reservoirs linked to reservoir age and latitude, *Nat. Geosci.*, doi:10.1038/NGEO1211.

Bertilsson, S., and L. J. Tranvik (1998), Photochemilly produced carbosylic acids as substrates for freshawater bacterioplankton, *Limnol. Oceanogr.*, *43*(5), 885–895.

Carignan, R. (1998), Automated determination of carbon dioxide, oxygen, and nitrogen partial pressures in surface waters, *Limnol. Oceanogr.*, *43*(5), 969–975.

Cole, J., and N. F. Caraco (1998), Atmospheric Exchange of carbon dioxide in a low-wind oligotrophic lake measured by the addition of SF6, *Limnol. Oceanogr.*, *43*(4), 647–656.

Cole, J. J., N. F. Caraco, G. W. Kling, and T. K. Kratz (1994), Carbon dioxide supersaturation in the surface waters of lakes, *Science*, *265*, 1568–1570.

Cole, J. J., et al. (2007), Plumbing the global carbon cycle: Integrating inland waters into the terrestrial carbon budget, *Ecosystems*, *10*, 171–184.

Crusius, J., and R. Wanninkhof (2003), Gas transfer velocities measured at low wind speed over a lake, *Limnol. Oceanogr.*, *48*(3), 1010–1017.

De Moortel, I., S. A. Munday, and A. W. Hood (2004), Wavelet analysis: The effect of varying basic wavelet parameters, *Sol. Phys.*, *222*, 203–228.

DeGrandpre, M. D., T. R. Hammar, S. P. Smith, and F. L. Sayles (1995), In situ measurements of seawater pCO_2, *Limnol. Oceanogr.*, *40*, 969–975.

DeGrandpre, M. D., D. W. R. Wallace, and C. D. Wirick (1997), Simultaneous mooring-based measurements of seawater CO_2 and O_2 of Cape Hatteras, North Carolina, *Limnol. Oceanogr.*, *42*, 21–28.
DeGrandpre, M. D., M. M. Baehr, and T. R. Hammar (1999), Calibration-free optical chemical sensors, *Anal. Chem.*, *71*, 1152–1159.
del Giorgio, P. A., and P. J. le B. Williams (Eds.) (2005), *Respiration in Aquatic Ecosystems*, Oxford Univ. Press, Oxford, U. K.
del Giorgio, P. A., J. J. Cole, and A. Cimbleris (1997), Respiration rates in bacteria exceed phytoplankton production in unproductive aquatic systems, *Nature*, *385*, 148–151.
Downing, J. A., J. J. Cole, J. J. Middelburg, R. G. Striegl, C. M. Duarte, P. Kortelainen, Y. T. Prairie, and K. A. Laube (2008), Sediment organic carbon burial in agriculturally eutrophic impoundments over the last century, *Global Biogeochem. Cycles*, *22*, GB1018, doi:10.1029/2006GB002854.
Durocher, Y.-D., et al. (2012), Reconciling the temperature dependence of respiration across timescales and ecosystem types, *Nature*, *487*(7408), 472–476, doi:10.1038/nature11205.
Emery, W. J., and R. E. Thomson (2004), Data analysis methods in physical oceanography, 2nd ed., Elsevier B.V.
Eugster, W., G. Kling, T. Jonas, J. T. McFadden, A. Wúest, S. MacIntyre, and F. S. Chapin III (2003), CO_2 exchange between air and water in an Arctic Alaskan and midlatitude Swiss lake: Importance of convective mixing, *J. Geophys. Res.*, *108*, 4362, doi:10.1029/2002JD002653.
Finlay, C. F. (2003), Controls of streamwater dissolved inorganic carbon dynamics in a forested watershed, *Biogeochemistry*, *62*, 231–252.
Grinsted, A., J. C. Moore, and S. Jevrejeva (2004), Application of the cross wavelet transform and wavelet coherence to geophysical time series, *Nonlinear Processes Geophys.*, *11*, 561–566.
Hanson, P. C., D. Bade, S. R. Carpenter, and T. K. Kratz (2003), Lake metabolism: Relationships with dissolved organic carbon and phosphorus, *Limnol. Oceanogr.*, *48*(3), 1112–1119.
Hanson, P. C., S. R. Carpenter, D. E. Armstrong, E. H. Stanley, and T. K. Kratz (2006), Lake dissolved inorganic carbon and dissolved oxygen: Changing drivers from days to decades, *Ecol. Monogr.*, *76*(3), 343–363.
Hoppe, H.-G., K. Gocke, R. Koppe, and C. Begler (2002), Bacterial growth and primary production along a north-south transect in the Atlantic Ocean, *Nature*, *416*, 168–71.
Huotari, J., A. Ojala, E. Peltomaa, J. Pumpanen, P. Hari, and T. Vesala (2009), Temporal variations in surface water CO_2 concentrations in a boral humic lake base on high-frequency measurements, *Boreal Environ. Res.*, *14*(suppl. A), 48–60.
IPCC (2007), *Climate Change 2007: Synthesis Report*, 52 pp., Intergovernmental Panel on Climate Change, Geneva.
Jennings, E., S. Jones, L. Arvola, P. A. Staehr, E. Gaiser, I. D. Jones, K. C. Weathers, G. A. Weyhenmeyer, C. Y. Chiu, and E. Eyto (2012), Effects of weather-related episodic events in lakes: And analysis based on high-frequency data, *Freshwater Biol.*, *57*, 589–601, doi:10.1111/j.1365-2427.2011.02729.x.
Jonsson, A., J. Åberg, and M. Jansson (2007), Variations in pCO_2 during summer in the surface water of an unproductive lake in northern Sweden, *Tellus B*, *59*, 797–803.
Kara, E. L., et al. (2012), Time-scale dependence in numerical simulations: Assessment of physical, chemical, and biological predictions in a stratified lake at temporal scales of hours to months, *Environ. Modell. Software*, doi:10.1016/j.envsoft.2012.02.014.
Kling, G. W., G. W. Kipphut, M. M. Miller, and W. J. O'Brien (2000), Integration of lakes and streams in a landscape perspective: The importance of material processing on spatial patterns and temporal coherence, *Freshwater Biol.*, *43*, 477–497.
Lewis, E., and D. W. R. Wallace (1998), Program developed for CO_2 system calculations, ORNL/CDIAC-105. Carbon Dioxide Inf. Anal. Cent. (CDIAC), Oak Ridge Natl. Lab., Oak Ridge, Tenn.
Millero, F. J. (1979), The thermodynamics of the carbonate system in sea- water, *Geochim. Cosmochim. Acta*, *43*, 1651–1661.
Nasseli-Flores, L. (2003), Man-made lakes in Mediterranean semi-arid climate: The strange case of Dr Deep Lake and Mr Shallow Lake, *Hydrobiologia*, *506-509*, 13–21.
Read, J. S., D. P. Hamilton, I. D. Jones, K. Muraoka, L. A. Winslow, R. Kroiss, C. H. Wu, and E. Gaiser (2011), Derivation of lake mixing and stratification indices from high-resolution lake buoy data, *Environ. Modell. Software*, *26*, 1325–1336, doi:10.1016/j.envsoft.2011.05.006.
Rimmer, A., Y. Aota, M. Kumagai, and W. Eckert (2005), Chemical stratification in thermally stratified lakes, a chloride mass balance model, *Limnol. Oceanogr.*, *5*, 147–157.
Roland, F., L. O. Vidal, F. S. Pacheco, N. O. Barros, A. Assireu, J. P. H. B. Ometto, A. C. P. Cimbleris, and J. J. Cole (2010), Variability of carbon dioxide flux from tropical (Cerrado) hydroelectric reservoirs, *Aquat. Sci.*, doi:10.1007/s00027-010-0140-0.
Romero-Martínez, L., M. Morales-Pineda, B. Úbeda, S. A. Loiselle, A. Cózar, and J. A. Gálvez (2013), Planktonic community metabolism in two stratified Mediterranean reservoirs with different trophic status, *Aquat. Ecosyst. Health Manage.*, *16*(2), 183–189.
Sadro, S., C. E. Nelson, and J. M. Melack (2011), Linking diel patterns in community respiration to bacterioplankton in a oligotrophic high-elevation lake, *Limnol. Oceanogr.*, *56*(2), 540–550.
Sobek, S., L. J. Tranvik, and J. J. Cole (2005), Temperature independence of carbon dioxide supersaturation in global lakes, *Global Biogeochem. Cycles*, *19*, GB2003, doi:10.1029/2004GB002264.
St Louis, V. L., C. A. Kelly, E. Duchemin, J. W. M. Rudd, and D. M. Rosenberg (2000), Reservoir surfaces as sources of greenhouse gases to the atmosphere: A global estimate, *BioScience*, *50*, 766–775.
Staehr, P. A., J. P. A. Christensen, R. D. Batt, and J. S. Read (2012), Ecosystem metabolism in stratified lake, *Limnol. Oceanogr.*, *57*(5), 1317–1330, doi:10.4319/lo.2012.57.5.1317.
Takahashi, T., et al. (2002), Global sea-air CO_2 flux based on climatological surface ocean pCO_2, and seasonal biological and temperature effects, *Deep Sea Res., Part II*, *49*, 1601–1622.
Teodoru, C., Y. T. Prairie, and P. A. del Giorgio (2010), Spatial heterogeneity of surface CO_2 fluxes in a newly created Eastmain-1 Reservoir in Northern Quebec, Canada, *Ecosystems*, *14*(*1*), 28-46, doi:10.1007/s10021-010-9393-7.
Tokoro, T., H. Kayanne, A. Watanabe, K. Nadaoka, H. Tamura, K. Nozaki, K. Kato, and A. Negishi (2008), High gas-transfer velocity in coastal regions with high energy-dissipation rates, *J. Geophys. Res.*, *113*, C11006, doi:10.1029/2007JC004528.
Torrence, C., and G. P. Compo (1998), A practical guide to wavelet analysis, *Bull. Am. Meteorol. Soc.*, *79*, 61–78.
Tranvik, L. J., et al. (2009), Lakes and reservoirs as regulators of carbon cycling and climate, *Limnol. Oceanogr.*, *54*(6), 2298–2314.
Vachon, D., Y. T. Prairie, and J. J. Cole (2010), The relationship between near-surface turbulence and gas transfer velocity in freshwater systems an its implications for floating chamber measurements of gas exchange, *Limnol. Oceanogr.*, *55*(4), 1723–1732, doi:10.4319/lo.2010.55.4.1723.
Van de Bogert, M. C., D. L. Bade, S. R. Carpenter, J. J. Cole, M. L. Pace, P. C. Hanson, and O. C. Langman (2012), Spatial heterogeneity strongly affects estimates of ecosystem metabolism in two north temperate lakes, *Limnol. Oceanogr.*, *57*(6), 1689–1700.
Wanninkhof, R., and M. Knox (1996), Chemical enhancement of CO_2 exchange in natural waters, *Limnol. Oceanogr.*, *41*(4), 689–697.
Weiss, R. F. (1974), Carbon dioxide in water and seawater: The solubility of a non-ideal gas, *Mar. Chem.*, *2*, 203–215.
Zar, J. H. (1999), *Biostatistical Analysis*, 4th ed., 663 pp., Pearson Prentice-Hall, Upper Saddle River, New Jersey.